Void Closure in Complex Plasmas under Microgravity Conditions

A. M. Lipaev,[1] S. A. Khrapak,[2] V. I. Molotkov,[1] G. E. Morfill,[2] V. E. Fortov,[1] A. V. Ivlev,[2] H. M. Thomas,[2] A. G. Khrapak,[1] V. N. Naumkin,[1] A. I. Ivanov,[3] S. E. Tretschev,[3] and G. I. Padalka[4]

[1]*Institute for High Energy Densities, Russian Academy of Sciences, 125412 Moscow, Russia*
[2]*Max-Planck-Institut für extraterrestrische Physik, D-85741 Garching, Germany*
[3]*RSC Energia, 141070 Korolev, Russia*
[4]*Yu. Gagarin Cosmonaut Training Center, 141160 Star City, Russia*

(Received 12 February 2007; published 29 June 2007)

We describe the first observation of a void closure in complex plasma experiments under microgravity conditions performed with the Plasma-Kristall (PKE-Nefedov) facility on board the International Space Station. The void—a grain-free region in the central part of the discharge where the complex plasma is generated—has been formed under most of the plasma conditions and thought to be an inevitable effect. However, we demonstrate in this Letter that an appropriate tune of the discharge parameters allows the void to close. This experimental achievement along with its theoretical interpretation opens new perspectives in engineering new experiments with large quasi-isotropic void-free complex plasma clouds in microgravity conditions.

DOI: 10.1103/PhysRevLett.98.265006 PACS numbers: 52.27.Lw

Complex (dusty) plasmas are multicomponent systems consisting of several charged components (electrons, ions, and macroscopic grains) and one neutral component (neutral gas). The grains are highly charged by collecting plasma on their surface. Because of the macroscopic size, the grains can be easily visualized, and due to their large masses, the dynamical time scales associated with the grain component are relatively long. These features enable us to observe the kinetic properties of the grain component in real space and time, making complex plasmas very useful tool for fundamental research at the most elementary level.

A rich variety of interesting phenomena in complex plasmas has been investigated in detail in ground-based experiments including self-organization, phase transitions, fluidlike flows, new wave modes, and instabilities [1–7]. However, on Earth grains are dominated by gravity, which severely restricts the range of the phenomena and limits the plasma parameter regime, which is available for laboratory studies. Most of the systems investigated there have been strongly compressed, inhomogeneous in the vertical direction and anisotropic. Consequently, it was recognized quite early that microgravity experiments were needed to complement the laboratory research [8,9].

The Plasma-Kristall PKE-Nefedov facility [10] on board the International Space Station (ISS), operational since March 2001, has enabled the study of complex plasmas under microgravity conditions. The experimental results reported so far include the formation of localized crystalline structures [10], the investigations of complex plasma boundaries [11,12], coalescence of complex plasma fluids [13], grain transport properties [14,15], the excitation and analysis of low-frequency waves [16,17], the observation of dust-acoustic shocks [18], the decharging of complex plasma [19], and the discovery of a new charge-induced gelation phase transition [20].

One of the interesting phenomena revealed in the studies of complex plasmas produced in rf discharges under microgravity conditions is the formation of a ''void''—a region in the center of the discharge which is free of macrograins [10,21]. It was suggested that the reason for the void formation could be the ion drag force, which pushes the grains out of the center [22]. Quantitative agreement between this model and the observations has been obtained recently [23] due to theoretical advances, showing that the ion drag force can be more than a factor ten larger than had traditionally been believed [24].

In past experiments, voids were formed under most of the plasma conditions and they were thought to be an inevitable effect. In this Letter we present the first measurement of void closure in the PKE-Nefedov experiment and provide theoretical interpretation. The results indicate how to produce large void-free grain clouds and will be important in designing new experiments under microgravity conditions.

The PKE-Nefedov facility is a discharge chamber consisting of a glass box with two circular electrodes with a diameter of 4.2 cm separated by a distance of 3 cm. The rf discharge is generated in argon at a frequency of 13.56 MHz and a voltage applied to the electrodes up to 50 V. The coupling of the rf to the electrodes is in the push-pull mode. A complex plasma is generated by injecting a few million micron sized grains (melamine–formaldehyde spheres of 6.8 μm in diameter in this experiment) into the plasma chamber from one of the two dispensers mounted in the upper and lower electrodes. The grains form a cloud inside the bulk plasma and are illuminated by a thin ($\sim$150 μm) sheet of laser light (produced by a laser diode and cylindrical optics), which is perpendicular to the electrode system. The reflected light is observed by two monochromatic CCD video cameras with a field of view of

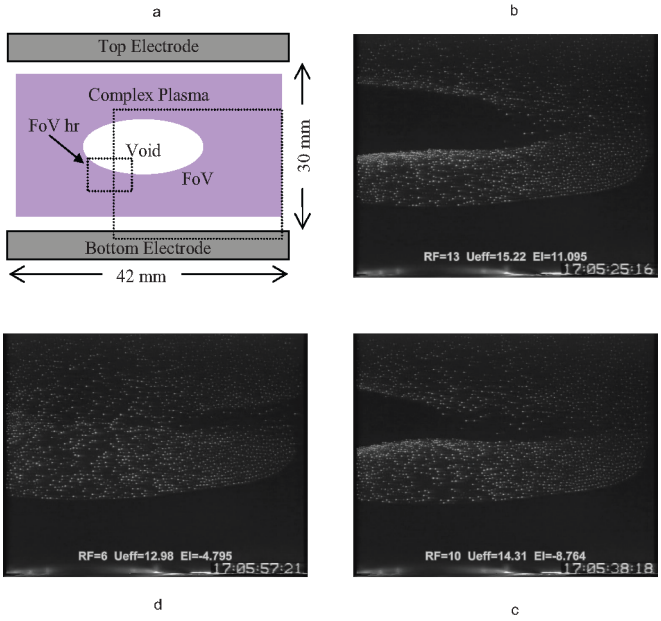

FIG. 1 (color online). Sketch of the experimental geometry (a); grain cloud, preelectrode sheaths, and central void (area free of grains) are shown schematically. The fields of view of the overview camera (FoV) and high resolution camera (FoV hr) are indicated, too. The figure also shows the different stages of the void closure: The void with maximal size (b), decreasing with decreasing of voltage (c), and vanishing at a voltage $U_{el} \approx 18$ V (d).

28.2×21.2 mm^2 (''overview'') and 8.55×6.5 mm^2 (''high resolution''), each with a rate of 25 frames per second. For the high resolution camera the pixel resolution is 11.8 μm/pixel. Both camera signals are recorded on video tapes. A schematic view of the experimental setup is shown in Fig. 1, more details can be found in Ref. [10].

The experiment was performed with argon gas at a pressure of 24 Pa. The discharge was switched on, particles were injected, and then, keeping the pressure constant, the electrode voltage was reduced stepwise. The evolution of the grain cloud is shown in Fig. 1. Figures (b),(c), and (d) correspond to the maximum voltage of $U_{el} = 21.5$, 20.2, and 18.3 V, respectively. By reducing U_{el} the grain cloud expands into the central region of the discharge and at some point void closure occurs [25].

A representative distribution of the grain density in the cloud along the vertical y axis of symmetry is shown in Fig. 2. This distribution was obtained by processing 100 video frames from the high resolution camera. The center of the chamber corresponds to $y = 0$. The void occurs in the region $y \lesssim 4$ mm. The boundary between the central void (i.e., conventional electron-ion plasma) and the complex plasmas is very sharp, which has been observed previously and explained by the formation of electric double layers [11]. The grain density experiences a maximum close to the inner complex plasma boundary and then decreases almost monotonically towards the outer cloud boundary where it again experiences an abrupt jump.

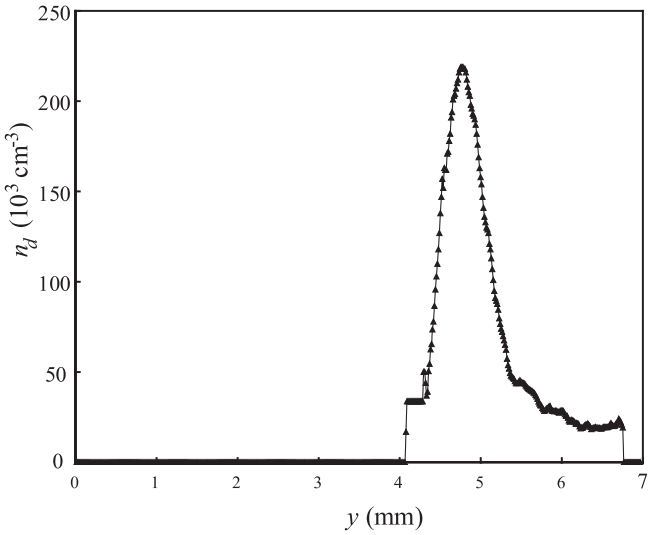

FIG. 2. The grain density distribution along the vertical y axis at a voltage $U_{el} = 23.7$ V.

The intergrain distance varies from ~370 μm at the outer boundary of the cloud to ~170 μm at the density maximum.

The dependence of the peak grain density (near the void boundary) and the void boundary position on the electrode voltage is shown in Fig. 3. At relatively high electrode voltages the peak grain density, n_{db}, exceeds the more typical value in the near constant density region further out, n_{dc}, by approximately a factor of 2. By reducing the electrode voltage U_{el}, the ratio n_{db}/n_{dc} increases and reaches a maximum value of ~10 at $U_{el} \approx 24$ V (see Fig. 3). The strong compression of the boundary region is evident. By reducing U_{el} further, the grain density near

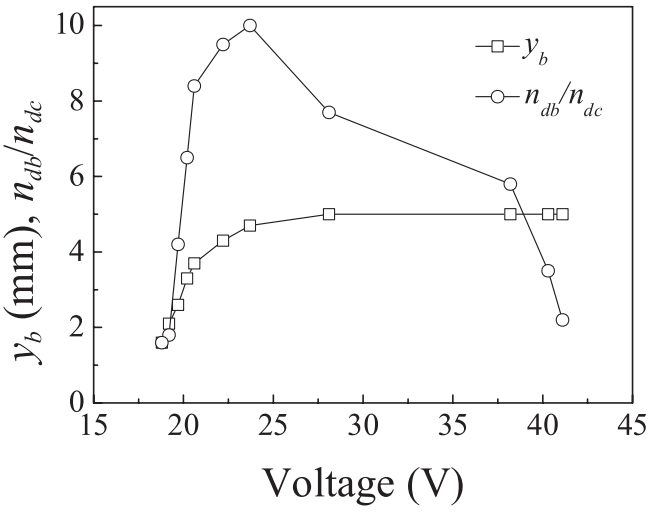

FIG. 3. The void boundary coordinate y_b and the ratio of the peak grain density near the boundary, n_{db}, to that inside the bulk cloud, n_{dc}, as a function of the voltage amplitude applied to the electrodes U_{el}.

the boundary decreases, and simultaneously, an expansion of the grain cloud into the central part of the discharge occurs. Note that the position of the outer grain cloud boundary is almost independent of the applied voltage.

Let us compare experimental results with theory. First, we briefly explain the mechanism responsible for the void formation. Imagine an *individual* grain in the central region of the discharge in the absence of gravity. The grain experiences two main forces. One is associated with the momentum transfer from the ions drifting from the center of the discharge to its walls and electrodes. This is the ion drag force, F_i, pushing the grain out of the center. The other is the electric force, F_e, which pushes the negatively charged grain towards the center. In some vicinity of the center the electric field E is weak, ion drift is subthermal, and ion drift velocity is proportional to the field, $u \propto E$. In this regime $F_i \propto u \propto E$ as well as $F_e \propto E$, making the force ratio F_i/F_e independent of the electric field. If the force ratio is larger than unity the grain cannot penetrate into the central part of the discharge where the electric field is weak. However, moving further to the periphery, the electric field increases and accelerates ions to suprathermal velocities. In this regime $F_e \propto E$, but $F_i \propto u^{-2} \propto E^{-1}$; i.e., the force ratio F_i/F_e decreases rapidly [26]. The balance condition $F_i = F_e$ determines stable equilibrium position of the grain and corresponds to the ''virtual'' void boundary.

When many grains are present in the discharge, the position of the actual void boundary and the structure of the grain cloud can be only approximately reproduced with the virtual void model outlined above. Main effects responsible for deviations are the internal (electrostatic) pressure of the grain component and the influence of the grains on the local plasma parameters, e.g., by elastic and inelastic ion-grain and electron-grain collisions. In principle, they can be consistently accounted for in numerical simulations [27]. However, in this Letter we do not attempt to describe the features of the grain cloud, but use a simpler approach. We analyze the ion drag-to-electrostatic force ratio F_i/F_e in the limit of vanishing field (i.e., representative to the central region of the discharge) to find conditions of the void formation or closure onset. The inequality $F_i/F_e > 1$ is a *necessary condition* for the central void formation, while the transition of the force ratio to values below unity would approximately indicate the condition of the void closure.

To calculate the ion drag force we use a model by Khrapak *et al.* [24], which extends the traditional Coulomb scattering theory to the regime of moderate ion-grain coupling. (Specifically, it takes into account that the characteristic length of the ion-grain interaction in complex plasmas can be larger than the plasma screening length, which requires a proper choice of the upper cutoff impact parameter, equal to the plasma screening length in the traditional Coulomb scattering theory). This model has been shown to agree reasonably well with the experimental results at low and moderate neutral gas pressures [28]. The expression for the ion drag force in the subthermal ion drift regime is [24]

$$F_i = (8\sqrt{2\pi}/3)a^2 n_i m_i v_{T_i} u[1 + \tfrac{1}{2}z\tau + \tfrac{1}{4}(z\tau)^2\Lambda], \quad (1)$$

where Λ is the *modified* Coulomb logarithm integrated over the Maxwellian distribution function of ions, $\Lambda \simeq 2z\int_0^\infty e^{-zx}\ln[1 + 2\tau^{-1}(\lambda/a)x]dx$, a is the grain radius, n_i, m_i, and $v_{T_i} = \sqrt{T_i/m_i}$ are the ion density, mass, and thermal velocity, $\tau = T_e/T_i$ is the electron-to-ion temperature ratio, $z = Ze^2/aT_e$ is the dimensionless grain charge (Z is the charge number), and λ is the effective plasma screening length, which is assumed to be close to the ion Debye radius. The ion drift velocity is calculated from $u = \mu E$, where $\mu \approx 7.2 \times 10^8$ cm/(V s) is the ion mobility in argon plasma [29].

To calculate the grain surface potential we equate the ion and electron fluxes which the grain collects from the surrounding plasma. For the electrons the standard orbital motion limited (OML) approach is used, while for the ions the effect of ion-neutral collisions, which can considerably affect their flux to the grain [30–34], is taken into account. The corresponding equation for the dimensionless charge yielding good agreement with the charges determined experimentally in a wide range of neutral gas pressures [34] is

$$v_{T_e}\exp(-z) = v_{T_i}[1 + z\tau + \xi^3(\lambda^3/a^2\ell_i)], \quad (2)$$

where ξ is the root of the transcendental equation $z\tau\exp(-x) = x(\lambda/a)$. The calculated values of the charge numbers are in the range from $Z \approx 7 \times 10^3$ to $Z \approx 1.6 \times 10^4$. The electric force is then calculated from $F_e = ZeE$.

The bulk plasma parameters are calculated using a 2D numerical code, SIGLO-2D [35]. The calculations are per-

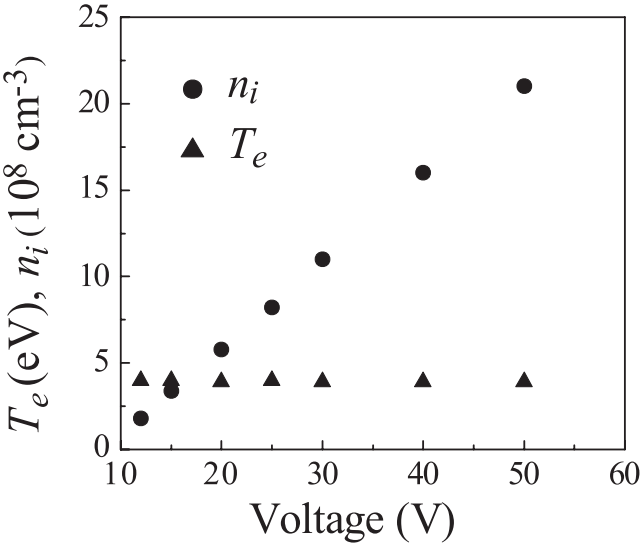

FIG. 4. The plasma density $n_i \approx n_e$ and the electron temperature T_e in the discharge center versus the voltage amplitude on electrodes, U_{el}.

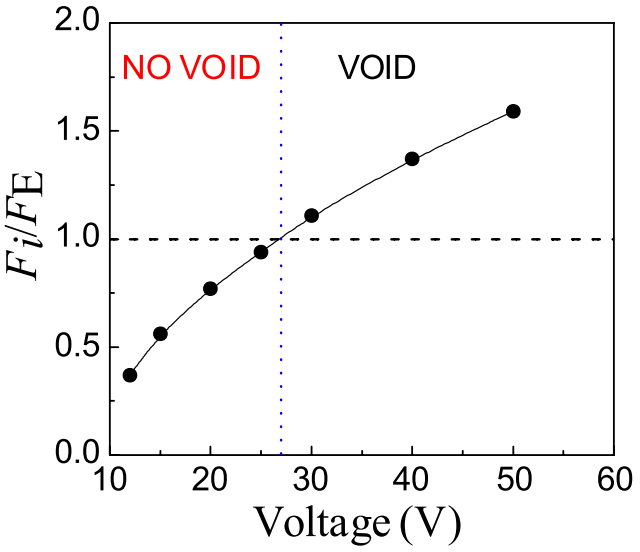

FIG. 5 (color online). The ratio of the radial ion drag and electric forces in the central region of the discharge (corresponding to the weak electric field) as a function of the voltage amplitude on electrodes, U_{el}.

formed for different values of the voltage applied to the electrodes at a fixed pressure of 24 Pa and using the same discharge geometry as in the PKE-Nefedov chamber. The values of the ion density and electron temperature in the center of the discharge are shown in Fig. 4. We see that $T_e \approx 4$ eV is almost independent of the applied voltage, while n_i increases almost linearly with U_{el}. The influence of the grains on the global plasma parameters is expected to be small since total plasma loss rate on the grains is estimated to be considerably smaller than the ionization rate within the discharge chamber. (This, however, does not exclude modification of the local plasma parameters inside the grain cloud.)

The calculated results of the force ratio F_i/F_e in the central part of the discharge are shown in Fig. 5. The force ratio decreases with reducing applied voltage and passes below unity at $U_{el} \approx 25$ V, in full qualitative agreement with our experiment. The quantitative agreement is also rather good—taking accuracy of the estimated plasma parameters, the model approximations, and some (unavoidable) effects of grains on plasma parameters (not considered in the SIGLO-2D code) into account.

To conclude, we have demonstrated experimentally the possibility of producing void-free complex plasmas under microgravity conditions. The main requirements are sufficiently low discharge pressures and very low voltages applied to the electrodes (close to the plasma-off conditions). The qualitative explanation is as follows: the plasma density decreases almost linearly as the rf voltage is reduced, leading to an increase of the screening length and decrease of the grain charge (due to enhanced ion collisionality). This implies that the ratio of the ion drag-to-electrostatic forces, which is a (slowly) increasing function of the factor $Ze^2/T_i\lambda$ in the limit of vanishing field [24], decreases. When this ratio drops below unity the net force acting on the grains is directed inwards and moves them into the central part of the discharge, where only the internal (electrostatic) pressure acts against this confinement; void closure occurs.

This work was supported by DLR/BMBF Grants No. 50WM9852 and No. 50WP0203, and by RFBR Grant No. 06-02-08100. The authors acknowledge excellent support of the PKE-Nefedov team.

[1] V. N. Tsytovich, Phys. Usp. **40**, 53 (1997).
[2] P. K. Shukla and A. A. Mamun, *Introduction to Dusty Plasma Physics* (Institute of Physics Publishing, Bristol, 2002).
[3] V. E. Fortov *et al.*, Phys. Usp. **47**, 447 (2004).
[4] R. L. Merlino and J. A. Goree, Phys. Today **57**, No. 7, 32 (2004).
[5] S. V. Vladimirov and K. Ostrikov, Phys. Rep. **393**, 175 (2004).
[6] V. E. Fortov *et al.*, Phys. Rep. **421**, 1 (2005).
[7] H. Thomas and G. Morfill, Nature (London) **379**, 806 (1996).
[8] H. Thomas *et al.*, Phys. Rev. Lett. **73**, 652 (1994).
[9] J. Maddox, Nature (London) **370**, 411 (1994).
[10] A. Nefedov *et al.*, New J. Phys. **5**, 33 (2003).
[11] B. M. Annaratone *et al.*, Phys. Rev. E **66**, 056411 (2002).
[12] P. M. Bryant, New J. Phys. **6**, 60 (2004).
[13] A. V. Ivlev *et al.*, New J. Phys. **8**, 25 (2006).
[14] V. E. Fortov *et al.*, Phys. Rev. Lett. **90**, 245005 (2003).
[15] V. E. Fortov *et al.*, Plasma Phys. Controlled Fusion **46**, B359 (2004).
[16] S. A. Khrapak *et al.*, Phys. Plasmas **10**, 1 (2003).
[17] V. V. Yaroshenko *et al.*, Phys. Rev. E **69**, 066401 (2004).
[18] D. Samsonov *et al.*, Phys. Rev. E **67**, 036404 (2003).
[19] A. V. Ivlev *et al.*, Phys. Rev. Lett. **90**, 055003 (2003).
[20] U. Konopka *et al.*, New J. Phys. **7**, 227 (2005).
[21] G. E. Morfill *et al.*, Phys. Rev. Lett. **83**, 1598 (1999).
[22] J. Goree *et al.*, Phys. Rev. E **59**, 7055 (1999).
[23] M. Kretschmer *et al.*, Phys. Rev. E **71**, 056401 (2005).
[24] S. A. Khrapak *et al.*, Phys. Rev. E **66**, 046414 (2002).
[25] Movies of the dynamics of the void closure in argon rf discharge are available from the web: www.ihed.ras.ru/animations/iss7_bp_244_4_sb_cut.avi.
[26] S. A. Khrapak *et al.*, Phys. Plasmas **12**, 042308 (2005).
[27] V. Land and W. J. Goedheer, New J. Phys. **8**, 8 (2006).
[28] V. Yaroshenko *et al.*, Phys. Plasmas **12**, 093503 (2005).
[29] L. S. Frost, Phys. Rev. **105**, 354 (1957).
[30] F. F. Chen, J. Nucl. Energy, Part C, Plasma Phys. Accel. Thermonucl. Res. **7**, 47 (1965).
[31] A. V. Zobnin *et al.*, JETP **91**, 483 (2000).
[32] M. Lampe *et al.*, Phys. Plasmas **10**, 1500 (2003).
[33] S. Ratynskaia *et al.*, Phys. Rev. Lett. **93**, 085001 (2004).
[34] S. A. Khrapak *et al.*, Phys. Rev. E **72**, 016406 (2005).
[35] J. P. Boeuf and L. C. Pitchford, Phys. Rev. E **51**, 1376 (1995).